RICE UNIVERSITY

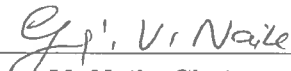# 1T-TaS$_2$ for Nonlinear Applications in Optical Neural Networks

by

Yuning Wang

A Thesis Submitted
in Partial Fulfillment of the
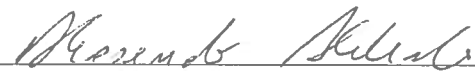Requirements for the Degree

Master of Science

Approved, Thesis Committee:

Gp', Vi Naik

Guruaj V. Naik, Chair
Assistant professor of Electrical and
Computer Engineering

Ashok Veeraraghavan
Associate Professor of Electrical and
Computer Engineering

Alessandro Alabastri
Texas Instruments Research Assistant
Professor of Electrical Engineering

Houston, Texas

October, 2019

ABSTRACT

1T-TaS$_2$ for Nonlinear Applications in Optical Neural Networks

by

Yuning Wang

Artificial neural networks (ANNs) is a kind of technology that simulates the human brain in order to realize artificial intelligence-like machine learning. This area keeps exploding recently and becomes powerful gradually. However, most of the approaches still rely on electronics, which come along with some natural limitations, like slow forward propagation and large power consumption. Optical neural networks (ONNs) is thought as a promising approach to overcome the shortcomings. Interference of lights can automatically offer floating-point computations. Linear transformation can be performed easily. Optical nonlinearities can be directly used to implement nonlinear activation functions. Besides, the architecture can be passive, and the speed is much higher. However, optical neural networks (ONNs) haven't been developed well. Most of the ONNs are still in the developing stage, and the nonlinear activation function has not been applied to real-word applications.

Tunable nanophotonics is one of the candidates to realize nonlinear activation functions in optical neural networks. However, the current tunability is either small or slow. Besides, it is tough to change the optical properties at room temperature with the small stimuli, which limits the nonlinear applications. Since some of the existing devices request strict experimental environments, researchers keep exploring new materials for better efficiency and lower cost. Here, we propose 1T-TaS$_2$, a

strongly correlated material for tunable nanophotonics. The optical properties of this material are susceptible to the external stimulus; that is, they have a large response to a small stimulus, which makes these materials promising in nonlinear applications.

TaS_2 is one kind of the Transition Metal Dichalcogenides (TMDs). TMDs are one of the strongly correlated materials involving abundant phases, such as the distorted phase, metallic phase, insulating phase, charge density wave (CDW) phase, superconducting phase and topological phase. Due to these different phases, TMDs exhibit possibilities for optical tunability. More attractively, $1T\text{-}TaS_2$ shows CDWs at room temperature, which means that its nonequilibrium states can be tuned under stimuli in a relatively easy way.

In this thesis, we propose that $1T\text{-}TaS_2$, whose optical properties can be tunable with white light at room temperature, is a promising material for nonlinear activation functions. We show that the refractive index of $1T\text{-}TaS_2$ can be tuned under white light excitation with intensities from 2.5 mW/cm^2 to 250 mW/cm^2. We also find that this tunability comes from the out-of-plane, not the in-plane, stacking difference of the material. By implementing this tunability, we design and simulate two nanophotonic nonlinear devices: angular modulation meta-grating and optical limiter. By changing the parameters of the device structures dynamically, we collect, analyze and summarize the simulation results to finalize the implementation of the most efficient devices that are meeting the expectations. And we find that by giving a specific structure, under different incident light intensities, the grating device can have a significant difference in the value of 6 degrees in the angle of reflected light. The reflective optical limiter can offer a reflection difference of more than 10% under different incident light intensities. The transmission of the transmitted optical limiter can reach 7% at the short wavelength range under different light intensities.

Acknowledgments

I have received supports, helps and directions from so many people, and it is hard for me to summarize all of them in a single paragraph. First, I would like to say thank you to Dr. Gururaj Naik for accepting me as his advisee and guide me in the research field. He opened the door to nanophotonics for me and led me to explore some inspiring research areas. Dr. Ashok Veeraraghavan helped me bring the marketing applications with my scientific work I was working on together. I would like to thank my committee members, Dr. Alessandro Alabastri, for his kind service.

Thanks to my friends in the Naik group, Chloe Doiron, Weijian Li, Sakib Hassan, Alex Hwang, Cameron Gutgsell, Frank Yang and Bob Bao. They helped a lot with my project and encouraged me to overcome any challenges I met during my research process. It is delightful and inspiring to work with them, both professionally and personally. Thanks to my friends, Yafei Wang, Weilu Gao, Xinwei Li, Minhan Lou. They never regretted to help me and answer my research questions. Thanks to all my friends at Rice University, you made me not feel lonely here. Thanks to the Department of Electrical and Computer Engineering, which provides a well-designed program for international graduate students and helps them to smooth the study experience at Rice University, as well as get used to the cultural difference in a different country. Thanks to Bella Martinez, a graduate project manager, she provided a lot of help for my study and life here and gave me enthusiastic support when I was depressed.

Special thanks to my husband, Zhuonan. Without his support, I will never be able to complete multiple challenging tasks together, which ultimately makes it an opportunity to defend the thesis. His understanding, which touches my soul deeply,

allows me to be the person I want to be and reach the dream that I should follow.

Contents

Illustrations

Chapter 1

Introduction

It has been a steady period of development for optical devices during the past decades. New designs and implementations come out each year in various industries and research fields. Managing the act of light has grown up to a well-defined field and has met the most needs in the industries around the world. However, due to the diffraction limit, conventional optical components, such as lenses and microscopes, often cannot focus light on the nanometer scale [4]. Recent developments in nanophotonic devices have clearly demonstrated the possibility of generating, manipulating, processing, transmitting, and detecting light in compact and highly integrated nanoscale structures, which is a new structure involved in many unresolved problems in reality. These devices hold high promises for providing another generation of breakthroughs needed for the photonics technology, together with a breakthrough for the productivity of the whole industry [5].

1.1   Tunable nanophotonics

Plasmonics is considered as one of the primary subfields of nanophotonics of light at the nanoscale. Plasmons are the collective oscillations of the electron gas in a metal or semiconductor [6]. Although many of the plasmonic structures are made of metals, such as gold and silver, those kinds of metal-based structures suffer from high losses of metals, heating, and incompatibility with complementary metal-oxide

semiconductor fabrication processes. On the other hand, there is another approach developed to manipulate nanoscale light with semiconductor particles, which can offer a longer carrier lifetime and provide the possibility for new innovative devices [7].

These well-structured optical devices provide the ability to perform optical experimental activities accurately and efficiently. However, in many of the situations, well-structured nano-optical devices are disadvantaged by the predefined structure and could not adjust to the needs to provide optical changes dynamically with a single device. Most of these materials also face limitations related to spectral tunability, lack of excitons at room temperatures, expensive fabrication processes, and low quantum yield [8]. There is still a journey to go for developing novel, efficient, tunable nanophotonic materials or devices. Tunable nanophotonic materials form the core of such devices, where a small change in optical constants of the material can produce a massive change in the overall functionality. Many such solid-state materials have been investigated for visible and near-infrared applications [9].

Many novel devices have been developed by extensive theoretical and experimental works, even though most of them are based on the photonic crystal structures designed to perform certain singleton functions without much less external control and adjustment. An innovative approach is needed to fully exploit the unique optical properties of photonic devices dynamically. Generally, there are four fundamental physical processes employed to trigger the targeted transient behavior, which could enable the tunability of the selected materials: electrical probing, optical pumping, mechanical actuation and chemical control [10].

As for the real-world applications, many tunable nanophotonic applications have been achieved in the real-world such as imaging, sensing, as well as optical modulation. However, none of each mechanism satisfies the requirements of the industrial

applications for the lack of either large or fast tunability. In an attempt to overcome such a limitation, electronically tunable optical materials whose optical properties are sensitive to a local electric field around room temperature are attracting increasing interests by researchers. Significant efforts have been contributed to the field of identifying specific materials to enable the electronic control of devices. By controlling the intrinsic optical properties of materials making up of nanodevices by electric fields, the amplitude and phase of excited light can be precisely adjusted [11].

Besides electronic control, remarkable results have also been delivered in terms of all-optical dynamic nanodevices. In the work of KF MacDonald and the co-workers, a demonstration of ultra-fast modulation of propagating surface plasmon polaritons is introduced. A femtosecond pulsed laser is used as both pump and probe. The optical signal coupled in and out from a plasmonic single interface waveguide by means of metallic grating [12]. Thus the optical properties of the device can be changed. When the goal is to maximize device performance in terms of speed, full optical control is usually performed. And most of the other devices with the same logic are making use of the change in the device properties in order to achieve the desired temporal variation of the optical properties.

There are some mechanically reconfigurable plasmonic structures serving as nanophotonic devices. One of the approaches is to use stretchable materials or micro-electromechanical system (MEMS) structures [13]. Stretchable films have been developed in order to enable a flexible shaping of the substrate. They are specifically important for their potential to develop wearable and personal optical devices [14]. The tunability could also be achieved by building plasmonic metasurfaces on top of the specific materials. For example, by building a beam-bending metasurface on top of a stretchable substrate, beam steering devices can be achieved [15].

The other commonly used approach to enable tunability for nanophotonic devices is chemical control. The basic idea of this approach is to find the specific materials, which are reversible in a phase transition to a particular reagent while remaining stable to other external chemical changes [10]. The previous research of Strohfeldt gives an identical example by finding a chemically mediated metal-dielectric phase transition in an array of yttrium dihydride [16].

1.2 Optical neural networks

There is also an increasing demand for research in the field of photonic neural networks [17]. As we all experienced, high-efficient computing architecture has become one of the most essential fundamentals of many industries in the past years. Since the microelectronics has been developed so well, industry engineers and designers were always able to implement the newest generation of electronic devices based on the newly-released microelectronic units. However, when it comes to a bottleneck of keeping adding additional structures on top of the original microelectronic designs, the exponential growth in transistor count and integration cannot be pushed further [18]. A widely used solution is to replace general processors and algorithms with Graphics Process Units (GPU) together with specific algorithms on top of that. One of the most commonly used algorithms is Neural Networks (NN), which is designed to simultaneously process a large volume of data in order to learn representations of the data with multiple layers of algorithms' abstraction. For each layer, there is a mechanism to collect the data array from the previous layer, process it in a single "neuron" by applying a nonlinear activation function for discriminating the data and transmit the result to the next layers of neurons [19].

Figure 1.1 shows a one-layer artificial neural network algorithm. Many nodes

are built into multiple layers, and this process is always simulated on hardware or by software. The input nodes are the initial message receivers. They will receive messages from external triggers, which, in most of the cases, are input data structures. Each node in the system represents a neuron body, getting a message, process it and deliver the generated results. The activation function employs a threshold or bias, and the connection weights act as synaptic junctions. As training data keeps going through, the learning occurs via the changes in the value of connection weights [20]. There is an example of a simple neural network algorithm, as shown in Figure 1.2. In this algorithm, the basic function of a neuron is to sum inputs and produce output if the given sum is greater than the threshold. There are two parts in the overall procedures: linear part and nonlinear part. The linear part is to receive the input signals V from neurons, sum the received data together and then add a linear bias bi.

$$z_i = b_i + \sum_j W_{ij} v_{ij} \tag{1.1}$$

The nonlinear part is to generate a new output signal by processing all the input signals through a nonlinear activation function.

$$a_i = \phi\left(z_i\right) \tag{1.2}$$

Thus, we will get the results, which are the numbers of sum outputs, with one additional criteria of a threshold limit.

Deep learning methods are representation-learning techniques obtained by composition of non-linear models that transform the representation at the previous level into a higher and slightly more abstract level in a hierarchical manner. The main idea is that by cascading a large number of such transformations, very complex functions can be learnt in a data-driven fashion using deep neural networks [21]. Applications of deep learning in multiple industries have realized huge success, especially in the
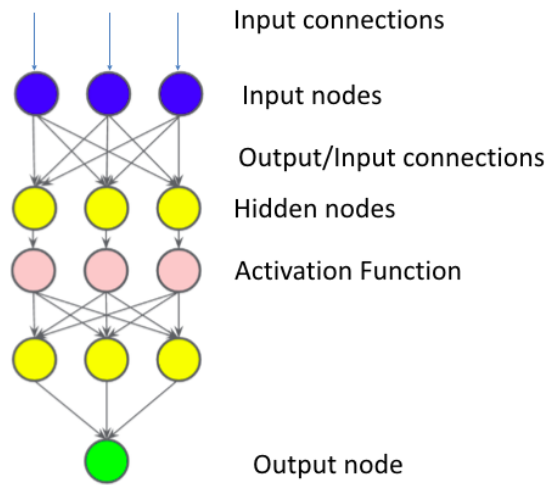
Figure 1.1 : A visual structure of the Neural Network algorithm.
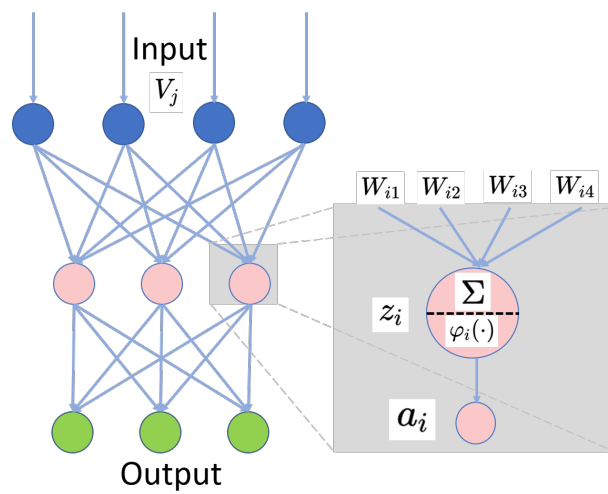

Figure 1.2 : A simple example of the Neural Network algorithm.

field of modelling complex input-output relationships. Similar logic could be easily applied to some other fields such as material design, computational imaging, and applied physics. It has received some attention in the optical community, and there have been several recent works on reverse modelling for the design of nanostructured optical components using NN, as well as hardware implementation of an artificial neural network [22]. NNs can be used to predict the optical response of a topology as well as to design a topology for a target optical response.

Even though the artificial neural network algorithms are placing and essential role in current industries, there are limitations for artificial neural networks (ANNs) to make a further step in development. Since the algorithms run on semiconductor-based hardware, the processing approaches will rely on electronic transport. Given the fact that computer performance is limited by energy dissipation and interconnect bandwidth density, it is hard to overcome the limitation in the electronic field. The source of nearly all energy dissipation is signal transmission in interconnects. And the interconnect bandwidth density is limited by resistance, capacitance, and wire interconnects geometry [23]. However, when it comes to the optical world, those limitations are different. Compared with electronics, the optics always has a very low energy dissipation. The light could provide a massive bandwidth in parallel by selecting wavelength and monitor combinations. Furthermore, devices based on optics could potentially achieve a high speed since processing with the speed of light [24].

In most of the cases, NN algorithms will take the majority of the processing time in the neuron processing stage. And by applying multiple layers of neurons, it means to multiply the processing time at a larger scale. While different from the traditional microelectronics elements, photonic devices could process predefined optical-based algorithms in the speed of light, which could be significantly faster than

the microelectronic approach when processing similar algorithms [25].

To demonstrate the general deep learning approach enabled by nanophotonics, there are a couple challenges to overcome. As described before, the NN algorithms require to apply a nonlinear activation function for discriminating the data. Thus a nanophotonic device providing the ability of nonlinear light properties is needed for the design. However, to the best of our knowledgethe experimental demonstration of optical neural network only contains the linear part [26], which is not sufficient to solve industry-level problems. Additionally, given the fact that we want to improve efficiency and reduce the cost by applying photonic NNs, the input and output light for the implemented device should be easily achievable and detectable, for example, visible light with the low illustration. To make the result detectable, we also need to find a proper index for the device and possibly using specific materials for building the structure.

Chapter 2

Choosing Nanophotonic Material

This chapter will briefly introduce the material candidates that can be used to achieve the desired nonlinear nanophotonic devices. The mechanism and physical theories will also be introduced.

2.1 Metal

Usually, metals such as gold, silver and Aluminum are chosen as Nanophotonic material. Surface plasmon resonance is a unique optical property of metal nanostructures. Plasmon is a subwavelength oscillating mode by coupling photons' energy with electron gas oscillation [6] [27]. Surface plasmon is the spread of the surface wave along a conductor. By changing the structure of the metal surface, the properties of surface plasmon polaritons (SPPs), the nature of the dispersion relation, excitation mode and coupling effect will have a significant change. Through the interaction between the light field and SPPs, active control of optical transmission can be implemented. With the development of nanotechnology, surface plasmon (SPPs) has been widely used in photonics. Therefore, metals form the dominating material used in the field of nanophotonics.

However, metals suffer from high losses, especially in the visible and ultraviolet (UV) spectral ranges, partly due to interband electronic transitions. Even the metals with the highest conductivities, gold and silver, have significant losses at optical

frequencies. These losses damage the performance of plasmonic devices, severely limiting the development of many plasmonic applications. Besides, incompatibility with complementary metal-oxide semiconductor fabrication processes also restricts the application of metal nanophotonic applications. Other disadvantages of metals include complex manufacturing, high cost, mechanical and chemical instability, and lack of sustainability at high temperatures. Besides all the challenges mentioned above, it should also be mentioned that metals' optical properties are not adjustable, which restricts their development in tunable nanophotonic devices.

2.2 Dielectric

Recently, dielectric materials with a high refractive index have attracted interest. Instead of plasma resonance in metal, dielectric materials offer strong, optically induced electric and magnetic Mie resonances [7]. The significant benefit of using dielectric materials is the low optical loss. Compared to plasmon resonance in metals, the bandwidth of Mie resonance in dielectrics may be much narrower. Besides, dielectric materials' compatibility with semiconductor device technologies is favorable. And they can generate both electric and strong magnetic resonances [28]. The abundant distinct optical resonances can provide more opportunities to realize different applications.

2.3 Semiconductor

The fabrication technology of semiconductor materials is mature and relatively easy, and their electronic and optical properties can be tuned in many ways. Different semiconductors can act with different resonance mechanisms. If the bandgap and plasma frequency of the semiconductor is larger than the interest frequency range, the semi-

conductor can also be treated as potential low-loss plasmonic material [29]. A large plasma frequency leads to a negative real permittivity, and a large bandgap means no loss due to transition losses. Also, Mie resonance can be realized in semiconductor materials [30].

2.4   2D Materials

Two-dimensional (2-D) materials have different physical and chemical properties with bulk three dimensional (3-D) materials. 2-D nonlinear optical material is an important element for the nonlinear nano-devices, so it has recently been widely concerned by researchers in optical, material, communication and medical field.

In recent years, scientists have discovered the ability to compress infrared light into two-dimensional materials such as graphene and hexagonal boron nitride (h-BN) to form surface plasma polaritons or phonon polaritons [31]. These polarons exhibit many excellent properties. For example, plasma polarons in graphene can be regulated by applying an electric field [32]. However, the fabrication technology of these materials is not yet mature; in-depth systematic research on the properties of materials is still lack. New materials are constantly emerging, but it is still an open proposition which material will dominate the new two-dimensional nonlinear optical materials in the future.

2.5   1T-TaS$_2$ - Strongly Correlated Material

Most 2-D materials, which get wide attention, are semiconductors, such as graphene, molybdenum disulfide (MoS$_2$) etc. However, strongly correlated 2-D materials are far from getting enough deserved attention. Compared to semiconductor and metal materials, the characteristics of strongly correlated materials are more complex. Strongly

correlated materials tend to be located near the boundary between metal and insulator. That is, electrons are between completely delocalized expanded states and completely localized energy levels. In semiconductor and metal materials, internal electronic movements can be considered independent, in which electrons do not affect each other. Unlike semiconductors and metals, there are strong interactions among electrons in strongly correlated materials. The strong interactions between electrons or between electrons and phonons cause many novel physical phenomena, such as superconducting metal-insulator transformation, quantum phase transition, etc.

To date, the strongly correlated electronic materials have been a hot spot and challenging point in the field of materials, optics, and physics. All disciplines are still cooperating in the research of this system to understand the complex physical phenomena of strongly correlated electronic materials, the physical mechanism behind them and the potential of their applications.

1T-TaS$_2$ is one kind of the Transition Metal Dichalcogenides (TMDs). The structure of TMDs can be represented as MX$_2$, with M representing transition metals (such as Mo, W, Ta, etc.) and X representing chalcogen elements (such as S, Se, Te). Due to the different atomic coordination of transition metal atoms, TMDCs hold two most common structural phases: trigonal prismatic (2H) and octahedral (1T). As shown in Figure 2.1, the difference of the monolayer TMDs' structure can also be seen as the difference of three atoms of surface layer (chalcogen - metal - chalcogen) stack sequence. 2H corresponds to ABA stacking, whose sulfur atoms of different atomic layers always occupy the same position A. In the direction perpendicular to the layer, each sulfur group is just in the lower sulfur group atoms of the upper part. And 1T corresponds to ABC stacking [33]. TMDs are one of the strongly correlated materials involving abundant phases, such as the distorted phase, metallic phase, insulating

phase, charge density wave (CDW) phase, superconducting phase and topological phase.
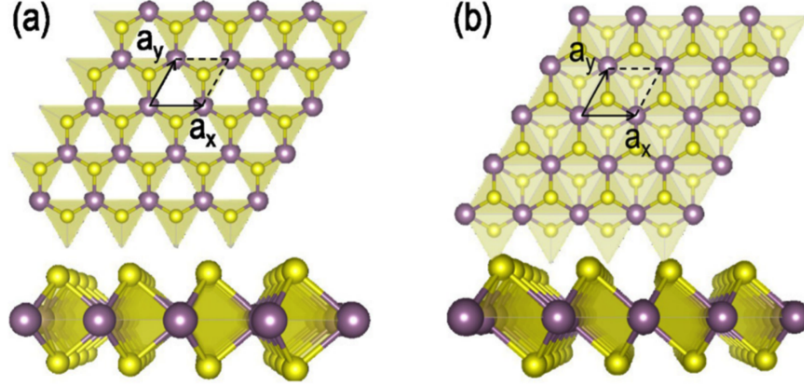

Figure 2.1 : Atomic structures of two TMD phases: (a) 2H, (b) 1T(Adapted from Ref. [1]).

Charge density wave (CDW) is a state with electron-density modulation in real space, which can be formed via several mechanisms. The effect electron-phonon coupling can renormalize the phonon dispersion, and in particular, the phonon mode can be softened (suppression of phonon frequency). The very strong suppression ultimately gives rise to the phonon spectrum instability, which leads to spontaneous deformation of the lattice. This event is known as the famous Peierls transition. It forms the lattice (atomic) density modulation in real space, and thus results in the formation of electronic CDW. In the CDW state, the material properties are susceptible to the external stimulus. That is, they have a large response to a small stimulus, which makes these materials very promising in tunable nanophotonic applications [34].

Usually, charge density waves happen at low temperatures [35]. However, 1T-TaS_2 can support it at room temperature. As shown in Figure 2.2, experimental results

show that 1T-TaS$_2$ has a rich phase transformation process at room temperature [2], from commensurate CDW (CCDW), nearly commensurate CDW (NCCDW) to incommensurate CDW (ICCDW).

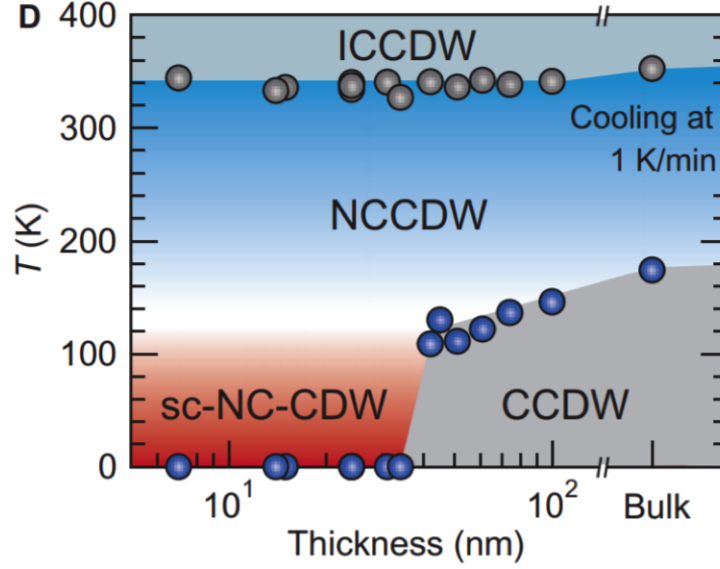Figure 2.2 : Phase diagram of 1T-TaS$_2$ nano-thick crystals with different thickness and temperatures(Adapted from Ref. [2]).

CDW phase of 1T-TaS$_2$ can be tuned by multiple stimuli, such as thickness tunability [2], gate doping tunability [36], pressure tunability [37] and strain tunability [38]. There have been some demonstrations of 1T-TaS$_2$, such as photoelectronic detectors [34], light tunable oscillators [39].

Chapter 3

Experiments

This chapter will introduce the detailed steps for preparing material 1T-TaS$_2$. It will also show the necessary analysis of the optical properties on the material.

3.1 Sample Preparation

In order to study the precise properties of 2D 1T-TaS$_2$, a simple and reliable method should be used to prepare the sample with specific size and surface properties. Because of the layered structure of 1T-TaS$_2$, mechanical exfoliation method was used. The bulk 1T-TaS$_2$ crystals were purchased from 2D Semiconductors Company.

Mechanical exfoliation is using transparency tape to break the van der Waals force between layers of crystal, without breaking the covalent bonds in the plane of each layer. In 2004, A.K.Geim [40] first proposed this method to get the single layer successfully. Currently optimized mechanical exfoliation method has been widely applied to the fabrication of other materials, such as h-BN, MoS$_2$, NbSe$_2$, etc [41]. Because no chemicals or chemical reactions are introduced in this method, the quality of the sample can be ensured. However, because this method is manually peeling, it has the disadvantages of low yield and low preparation efficiency, and the size, shape and thickness of the prepared 2D materials are not controllable.

In my experiments, the sample preparation process was mainly divided into the following steps:

1. Clean glass substrate. First, I cleaned the glass substrates by three 10-min ultrasonic clean using acetone, ethanol and deionized water in turn. Then dried the substrates with clean nitrogen stream. Next, I used plasma cleaner for 10 min (rice shared equipment) to clean them further.

2. Mechanical exfoliation. Adhere the bulk material to the tape, and then use another piece of the tape to adhere again. Repeating several times, adhere the tape to the glass substrate to get the 2D $1T\text{-}TaS_2$.

3. The thickness measurement. Thickness of the sample was measured by Atomic Force Microscope (AFM). The thickness of the sample with good quality is in the range of 10-200 nm.

3.2   Optical Characterization

Optical characterization was implemented with white light excitation and a microscope coupled to an imaging spectrophotometer. Figure 3.1 presents the schematic diagrams of the reflection and transmission spectrum measurement system. Here I used halogen tungsten lamp as the light source, whose output power is stable, and the spectrum is smooth. $1T\text{-}TaS_2$ thin film was put on the sample stage of the microscope (Eclipse Ti, Nikon). An objective with 1 NA and 60 magnification was chosen in order to collect more angles light. The reflection and transmission light were collected by a lens and focused at the slit of the CCD (Isoplane SCT320, Princeton Instrument) connected with a spectrometer (Pylon, Princeton Instrument).

When do the measurement, there are some points that should be noticed:

1. The CCD should work at low temperatures to avoid the effect of dark current noise.
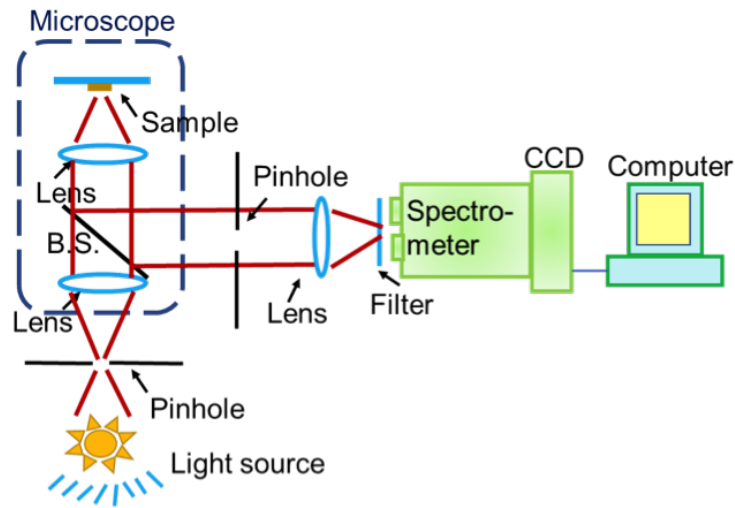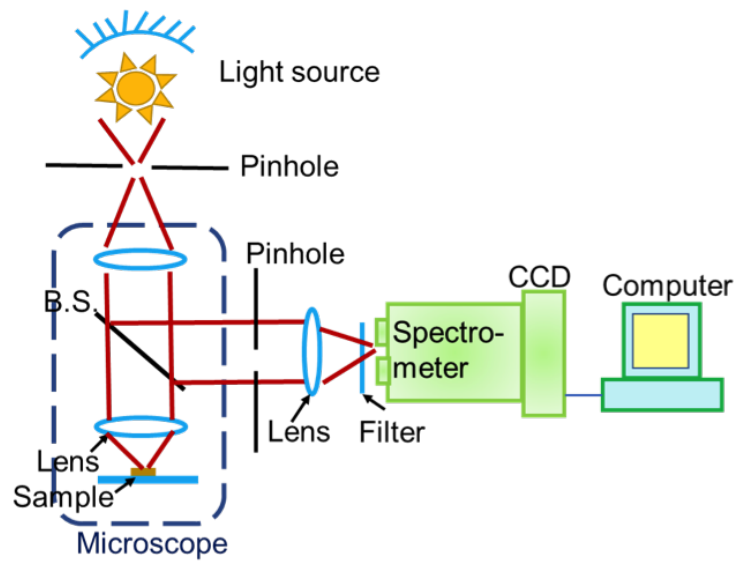
Figure 3.1 : The schematic diagram of (a) reflection setup; (b) transmission setup.

2. The background noise should be cancelled off.

3. It is necessary to select the corresponding filter in front of the slit of CCD according to the different measuring range, so as to eliminate the second-order

diffraction light.

Using the spectrum measurement system in Figure 3.1, First, we measured the reflection and transmission with a normal incident white light. The spectrum of a sample with an average thickness of 90nm is shown in Figure 3.2. The dielectric function (ε_0) was extracted at every single wavelength, as shown in Figure 3.3. Both the real part and the imaginary part of this material is relatively large. From the results, we can get the conclusion that 1T-TaS$_2$ is a high index absorption material in the visible range.
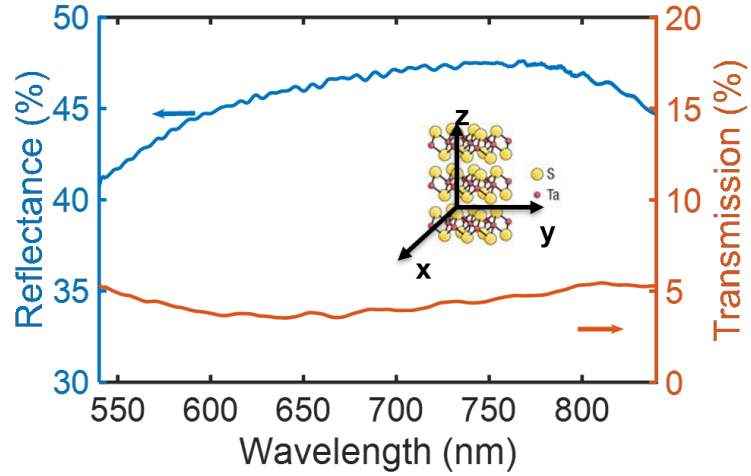
Figure 3.2 : Reflection and transmission spectra with normal incident white light.

As the degree of condensation of carries in 1T-TaS$_2$ is sensitive to the stimulus, we studied the optical properties of 1T-TaS$_2$ with different incident light intensities. We used different combinations of neutral density (ND) filters to adjust the incident white light intensity, with the range from 2 mW/cm^2 to 400 mW/cm^2. Because 2D materials hold anisotropy property [42], the optical properties should be expected with high direction-dependent properties.

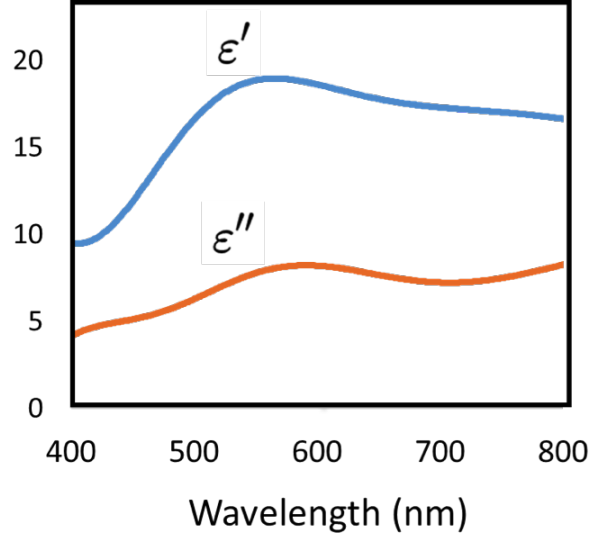Figure 3.3 : Dielectric function of 1T-TaS$_2$.

First, we used normal incident light with different intensities to measure the transmission and reflection spectra. The spectra were almost the same with different incident light intensities. Later, by changing the position of the pinhole in front of the CCD, a large angle of incident light was collected. We found that the transmission and reflection were changed with different incident light intensities. Figure 3.4 shows these changes at two incident intensities. The refractive index was extracted at every single wavelength, as shown in Figure 3.5. Only using the white light, both the real part and imaginary part of the refractive index could be changed. At 400nm, the change of real part could be around 0.3, which is huge compared to other exiting materials.
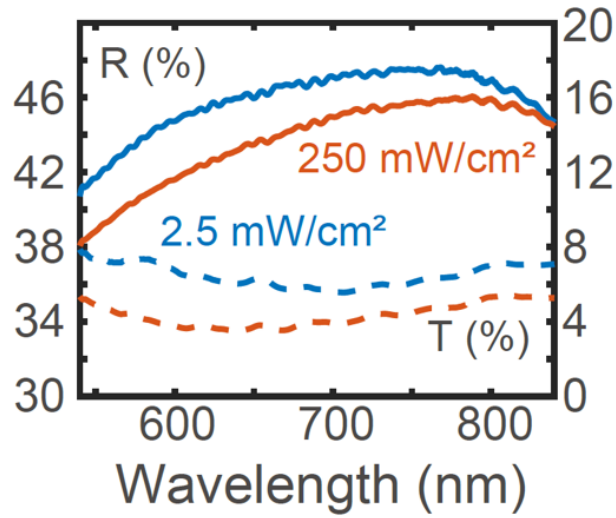
Figure 3.4 : Tunable optical properties of 1T-TaS$_2$ under the white light: reflection and transmission under the incident light intensities of 2.5 and 250 mW/cm^2.
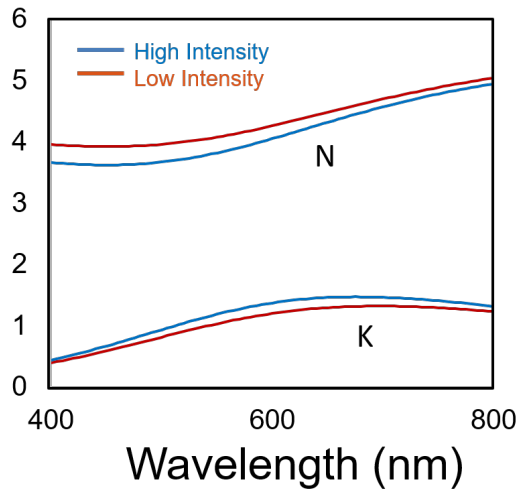

Figure 3.5 : Real part(N) and imaginary part(K) of the refractive index under the incident light intensities of 2.5 and 250 mW/cm^2.

Chapter 4

Nonlinear 1T-TaS$_2$ Devices

4.1   Angle-Tunable meta-Grating

Giving the concern that the degree of condensation of carriers in 1T-TaS$_2$ can be influenced by the external perturbation such as an electric field, experimental temperature and optical excitation [43], the optical properties could also be influenced. Based on the observation during the characterizations of 1T-TaS$_2$, we realized that the optical properties of this material are quite sensitive to the light intensity, which could even be at a very low illumination intensity around 100 mW/cm^2. In order to make the most of the optical tunability of 1T-TaS$_2$ and build nonlinear devices, which can be uesd as nonlinear activation function in optical neural networks, we proposed a tunable grating with intensity-dependent diffraction.

A diffraction grating is a structure that uses the optical principles of diffraction and interference. An ideal diffraction grating consists of a group of infinitely long and infinitely narrow slits with equal spacing, and the spacing between slits is d, which is called grating constant. When the plane wave of λ wavelength enters the grating at an angle θ_i, each point on the slit serves as a sub-wave source. The light emitted by these sub-sources travels in all directions (i.e., spherical waves). Since the slit is infinitely long, only the case on the plane perpendicular to the slit can be considered. That is, the slit can be reduced to a row of points on the plane. The light field in a particular direction on the plane is generated by the coherent superposition of the light emitted

from each slit. In the event of interference, some or all of the light emitted from each slit will cancel out, since the phase of the light emitted from each slit is different at the point of interference. However, interference intensification occurs when the difference between the light path from two adjacent slits to the interference point is an integral multiple of the wavelength of the light, and the two beams have the same phase. The grating equation can be written as:

$$d \left(sin\theta_m \ \pm \ \sin\theta_i \right) = \text{m}\lambda \tag{4.1}$$

where d is the diffraction constant, $\sin \theta_m$ is the diffraction angle; $\sin \theta_i$ is the incident angle. "+" is chosen when incident light and the diffraction light are on the same side of the normal line, "-" is chosen when the incident light and the diffracted light are on the other side of the normal line. λ is the wavelength, m is an integer with values of $0, \pm 1, \pm 2. \ldots$. This interference intensification point is called diffraction maximum. Therefore, when the diffraction angle satisfies the grating equation, the diffracted light will reach the maximum value. Figure 4.1 shows a grating schematic diagram.

Optical gratings are used for light coupling and delivery in a variety of optical systems. It is an optical transmission device with periodic or aperiodic regions with different refractive indexes in the direction of light propagation. As we learned that the optical property of $1T\text{-}TaS_2$ is quite sensitive to source light intensities and could provide a nonlinear reaction on the intensity changes, we could build a grating device on top of this material to increase the differentiation supporting the nonlinear activation function.

Figure 4.2 depicts a schematic of the grating-based device. As shown in the figure, the device was designed to base on a glass substrate. The glass surface is covered with

a silver mirror layer, which is covered with a thin Al_2O_3 protective layer. A proposed 50 nm of the 1T-TaS$_2$ layer is placed on the mirror layer. Finally, place silver slabs on the top layer with a proposed period of 400 nm.
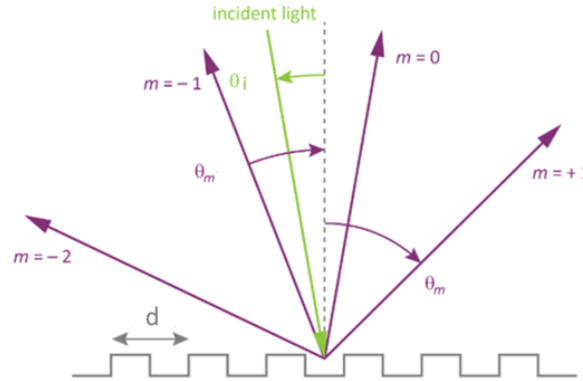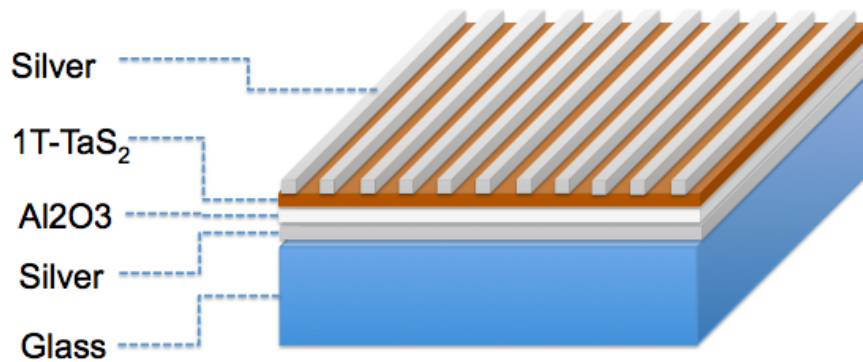

Figure 4.1 : The schematic diagram for grating.

Figure 4.2 : 3-D grating structure.

A 2-D Finite Difference Time Domain (FDTD) technique was used to model the structure of photonic gratings. As discussed in the previous section, the optical

property of the 1T-TaS$_2$ layer is supposed to be different with different source light intensities. The purpose of this FDTD design is to figure out the best combination of settings on the silver slabs.

Larger area device can offer higher accuracy and possibility for more applications. However, limited by the mechanical exfoliation of 1T-TaS$_2$, it is not easy to get a relatively large area thin film sample. Therefore, it is essential to have relatively small structures. According to the diffraction grating equation, a smaller wavelength indicates a smaller period. Hence, we chose 532 nm light as the incident light, which belongs to the visible light range and is relatively short-wavelength light, as the wavelength of our simulating source light. We chose 10 mW/cm$_2$ as the low incident light intensity and chose 500 mW/cm$_2$ as the high incident light intensity (this setting will apply to all the following experiments in this thesis). The refractive index used in this simulation refers to the present study of TaS$_2$ properties in our group [44].

In the simulation experiment, the incident plane wave was set as 532 nm, 45 incident angle, and the source type was BFAST, which is suitable for oblique incidence cases. The period was chosen as 400 nm or 500 nm. The width and thickness of the silver blank changed dynamically from 60 nm to 200 nm, and the difference is 20 nm. There were 64 combinations in total.

When it comes to the final simulation results, we used Matlab to extract and plot all the monitored results together, picking up the silver slab setting combination which brought the largest diffraction angle difference under different incident light intensities. As shown in Figure 4.3, the maximum angle difference of -1 order with different incident light intensities can be up to 6 degrees. The size of the silver slab is 120 nm width and 160 thickness, as shown in Figure 4.4.

For more comfortable usage and preparation, we prefer to place the monitor on

the other side of the source light. Therefore, the expected combination of the grating device will have a silver slab with a thickness of 160 nm and a width of 120 nm. We also tried to change the period dynamically but found no significant change on the largest angle difference of the monitoring result.
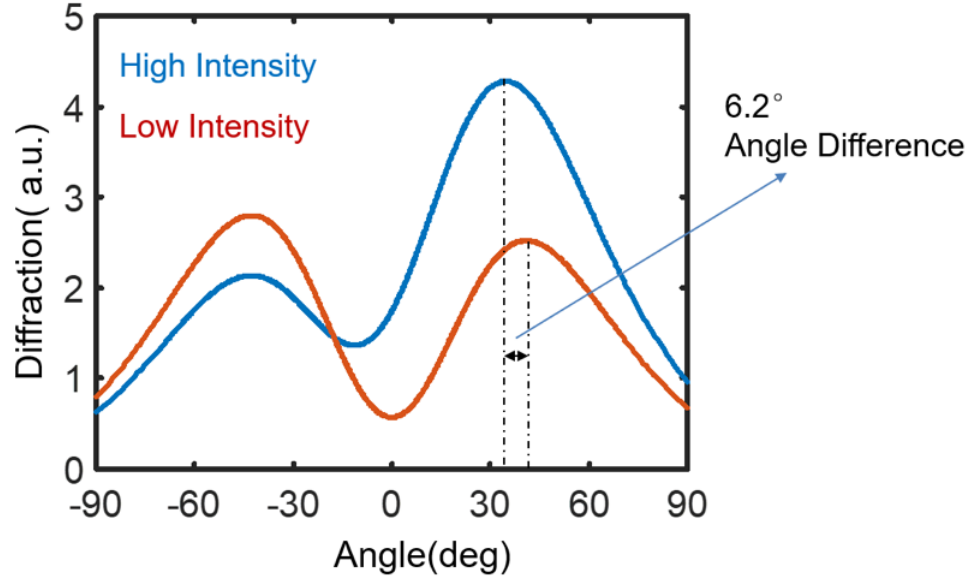
Figure 4.3 : Diffraction angles under different incident light intensities.

4.2 1T-TaS$_2$ Optical Limiters

The design of grating is to change the reflection angle based on the original reflection characteristics of the fundamental material. In order to change the refleaction and transmission behavior of the light source, we proposed another photonic device called an optical limiter (OL).

The optical limiter is widely used to protect optical sensors and receivers in the environments where there are high-intensity light sources. It has a low absorption rate

Figure 4.4 : Final grating structure in detail.

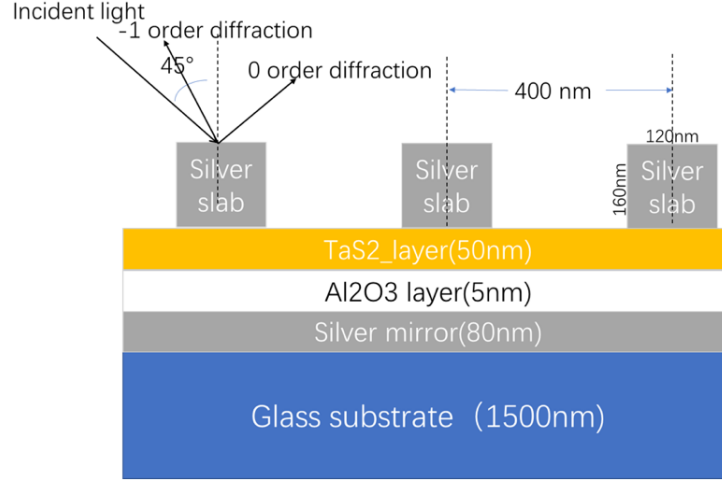at low light intensities and high absorption rate at higher intensities. Multiple non-linear processes could be utilized for optical limiting, including nonlinear scattering, absorption, refraction, and multiphoton absorption [45]. Nonlinear optical limiters provide an agile means of protection against pulsed lasers [46]. Nonlinear materials can take effect on the transmission of a strong light pulse, and limit the output to lower intensity levels. Protection is initiated by the device itself.

However, almost all existing nonlinear materials require a tightly focused beam to initiate the effect. Therefore, any limiter must be integrated into the optical system [45]. Currently, there are many nonlinear OL devices implemented in semi-conductors. Besides, the ability to provide a nonlinear reaction is closely related to near-band-gap resonance, and therefore nonlinear reaction lies in a region of relatively high linear absorption [47]. If we can find a material that can exhibit sensitivity to light intensity by itself, then we can use OL structure to increase the limiting effect

of the material.

Since 1T-TaS$_2$ is sensitive to the light intensities, we used it as the basement material to build an OL device to produce nonlinear responses. Here, we designed two optical limiter structures that provide relatively non-linear reflection and transmission behavior. Like the angle-tunable meta-grating discussed before, these optical limiters are also good candidates to serve as nonlinear activation functions in optical neural networks.

4.2.1 Reflective Optical Limiter

We used the thin-film structure to realize the reflective optical limiter. Changes in the complex refractive index of TaS$_2$ will change the reflectivity of a sample. This effect can be explained by destructive interference. This structure allows for the suppression of reflectivity ("enhanced absorption") through destructive interference between all the reflected partial waves, as shown in Figure 4.5 [3].

As a wave passes through the film, the amount of light phase it accumulates depends on what is called "optical thickness," which is a function of the thickness of the layer, the angle of incidence, and the refractive index. Thus, the destructive and constructive interference conditions depend on the refractive index of the film and the surrounding area, the thickness of the film, and the angle of view.

Figure 4.6 shows a schematic of the device structure. The whole device is designed on a 1500 nm thick glass substrate. On top of the glass, there is an 80 nm silver mirror layer covered with a 5 nm Al$_2$O$_3$ protective layer, then a 1T-TaS$_2$ thin layer.

A 3-D FDTD method was used to model the structure. As discussed in the previous section, the optical property of the 1T-TaS$_2$ layer is supposed to be different with different source light intensities. The purpose of this FDTD design is to figure
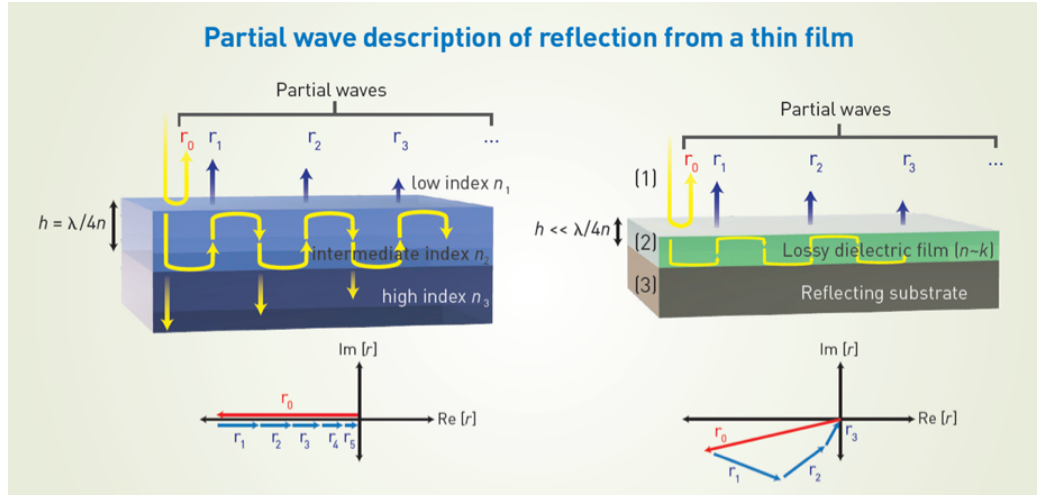
Figure 4.5 : Partial wave presentation in two thin film structures. (Left) Conventional 1/4 wave anti-reflection thin film. (Right) Reflection suppression using an ultra-thin, lossy layer on a reflecting substrate(Adapted from Ref. [3]).

Figure 4.6 : Optical Limiter structure in detail.

out a proper 1T-TaS$_2$ thickness, which can produce a higher rate on the reflection difference given different input light intensities. We set the simulating source light range to be between 400 nm to 1000 nm. By changing the thickness of 1T-TaS$_2$ layer

dynamically, we can observe and analyze the result on reflection.

Figure 4.7 shows the results of different thickness options. We can observe that the reflection behavior of the device varies significantly with the thickness of the material. With a 5 nm 1T-TaS$_2$ layer, the reflection of high incident light intensity is larger than that with low incident light intensity, which cannot "limit" light. With a 10 nm 1T-TaS$_2$ layer, at the wavelength range from 400 nm to 450 nm, the reflection of high incident light intensity is lower than that with low incident light intensity, which first realizes the function of optical limiter. With a 15 nm 1T-TaS$_2$ layer, the reflection difference between different incident light intensities can reach 15% and has a broadband working wavelength range. By increasing the thickness of the 1T-TaS$_2$ layer, the working wavelength range is expanding, but the difference of reflection is decreasing. And the absolute reflection also changes. Taking all the elements into consideration, we could get the ideal structure with a 30 nm 1T-TaS$_2$ layer. The reflection is relatively high with both low and high intensity incident light. The max difference of reflection with different given light intensities is 12%. The working wavelength range covers all visible light.

4.2.2 Transmitted Optical Limiter

The transmitted optical limiter was designed based on the Fabry-Perot effect. The Fabry-Perot cavity example is one of the most straightforward optical resonator structures. In optics, the Fabry Perot interferometer is a multi-beam interferometer consisting of two parallel glass panels, both of which are highly reflective relative to the inner surface. For the Fabry-Perot structure, the significant change of transmittance with wavelength is due to the interference of multiple reflected lights between two reflective plates. When the transmitted light is in the opposite phase, the minimum

transmittance is realized. When the numerous reflected lights are in the same phase, the maximum is realized. The Fabry-Perot resonance depends on the wavelength of the incident light, thickness between two layers and the refractive index of the material.

Figure 4.8 shows the device structure. Here, we chose TiO_2, which is a high refractive material with relatively less loss dielectric material, to realize the Fabry-Perot effect. When light is incident on a certain thickness of TiO_2, which meets the phase request, the Fabry-Perot interference effect will occur. By adding a 1T-TaS_2 layer in the center of TiO_2, we can realize to change the refractive index of the material by different incident light intensities and further change the Fabry-Perot resonance.

In the FDTD simulation experiment, the source was set as a normal incident plane wave light in the visible range. By changing the thickness of the TiO_2 layer and 1T-TaS_2 layer dynamically, we found that the transmission of high intensity incident light could be less than that of low intensity incident light. As shown in Figure 4.10, the difference could reach 7% at the short wavelength range. This result comes from the structure shown in Figure 4.9.
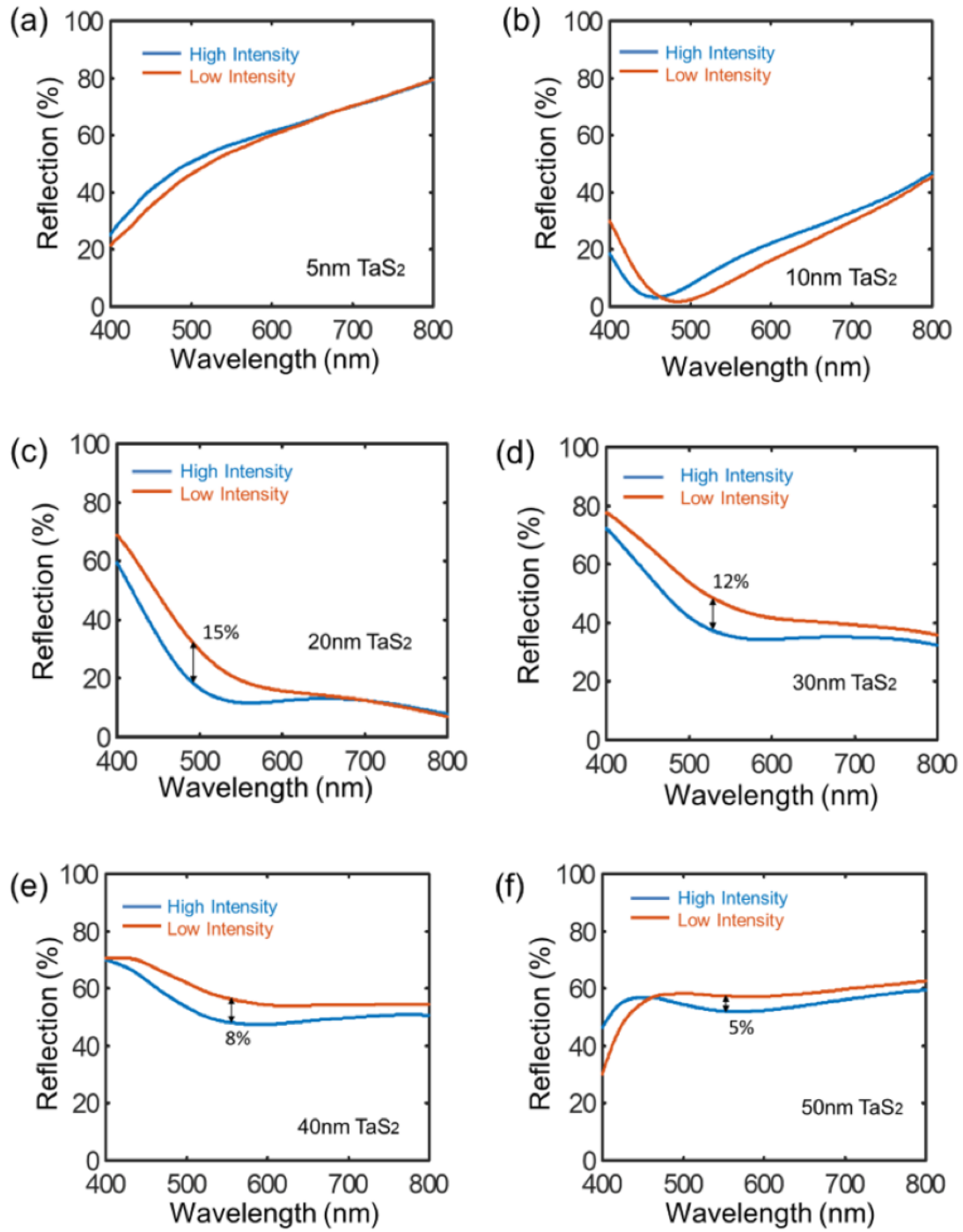
Figure 4.7 : Reflection under different incident light intensities with different thicknesses of the TaS$_2$ layer.
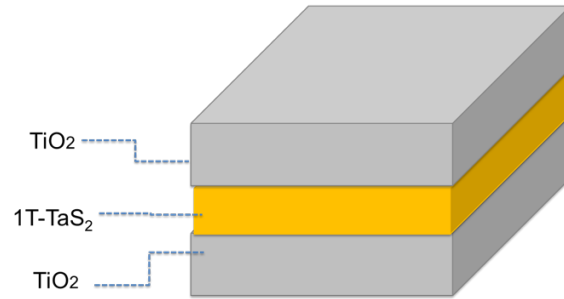
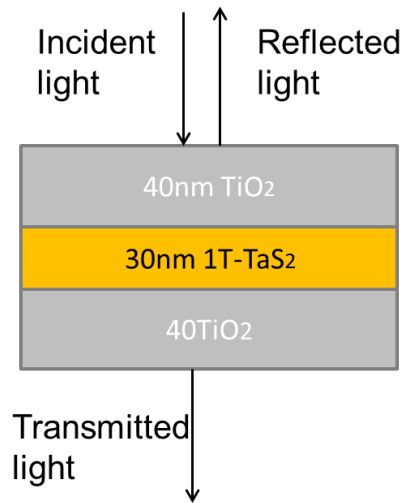Figure 4.8 : Transmitted Optical Limiter 3-D structure.

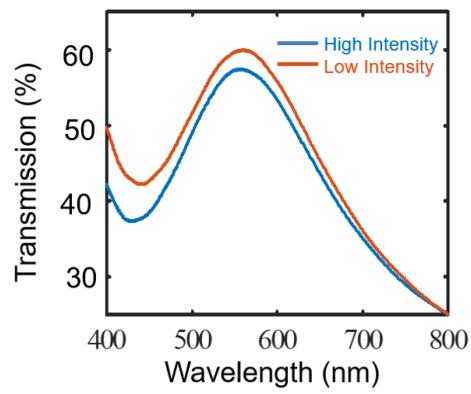Figure 4.9 : Optimized transmitted Optical Limiter structure.

Figure 4.10 : Transmisson under different incident light intensities.

Chapter 5

Conclusion

5.1   Research Summary

In this thesis, we explored briefly on the development of nanophotonics and artificial neural networks. We shared our motivations by linking the two research fields together and tried to overcome the bottlenecks limited by electronic fundamentals, with the application of nanophotonic devices for the neural network implementation. Since optics has the advantages of parallel processing, lower energy dissipation and bandwidth throughput over electronics, what we are looking for is a photonic device to provide a nonlinear activation function, which can be used to implement the neural network algorithms.

In order to have a proper design on the optical devices, we introduced and prepared the nanophotonic material 1T-TaS$_2$. It provides a specific ability to change its optical properties by giving different light intensities. Based on the material, we designed two optical devices. The grating design is able to provide a nonlinear relationship by having different reflection angles with different input light intensities. And the optical limiter design, on the other hand, shows the nonlinear functionality by giving nonlinear reflection or transmission rates with different input light intensities. Both devices were designed at the nanometer level. They are suitable for use as a basic device for building photonic neural networks.

5.2 Contributions and Limitations

This study makes three major contributions. First, it proposes and clarifies a theoretical grounded conceptualization of nanophotonics and why photonics should be applied to the field of neural network research. As discussed in previous sections, the critical point of linking these two research fields together is to achieve a nonlinear activation function with optical devices, instead of general electronic devices. Second, in order to obtain the nonlinear characteristics, this thesis explores the $1T\text{-}TaS_2$ material. The theoretical fundamentals are well presented. And the experiments are explained in detail about the steps to prepare $1T\text{-}TaS_2$. The general optical properties of this material are also analyzed in the characterization experiments. The last contribution is to design and simulate nanophotonic devices based on $1T\text{-}TaS_2$. By making use of the feature of being sensitive to light intensity changes, these devices are able to provide the ability to react to the light source with nonlinear response. For the grating structure, it is based on the reflection angle difference, and the optical limiters react with different reflection and transmission rates, respectively. These two approaches can potentially meet different kinds of nonlinear function requirements. The nanophotonic devices designed in this thesis also have gentle environment requirements of room temperature and visible source light.

As for limitations, this study is currently focusing on the simulation design and implementation of the nanophotonic devices. When it comes to reality, due to the restrictions of actual experiments or the accuracy of simulations based on ideal conditions, it may bring new challenges. This thesis does not implement the actual photonic neural network functionality since the time and research devices are restricted. There are also limitations to the optical neural network itself, which is currently performing well in object classification but not the other machine learning tasks [19].

5.3   Future Research

Upon the conclusions of this study, several areas of further research can be addressed. As the fundamental material is well designed and prepared, future research should continue with the implementation of these nanophotonic devices. We should test the performance of the equipment in normal experimental environments. Based on the finalization of the actual devices, we can start designing and implementing the neural network models in the following experiments.

Chapter 6

Supplemental Material

6.1   Grating Simulation Result Analysis

With the plane wave type of periodic and the receiving monitor on the other side to the source light, we could achieve the most significant difference on the reflection light angles with 160 nm in thickness and 120 nm in width. The angle difference of this combination is 6.20 degrees. When changing the plane wave type to BFAST, the combination above also provided a difference greater than 95% of the other combinations. The angle difference was 0.98 degrees. Once we changed the receiving monitor to the same side of the source light, the best combination for periodic plane wavelength would be 160 nm in thickness and 120 nm in width, providing a 3.49 degrees difference. The BFAST source with the same combination will provide a 0.98 degrees difference, which is greater than 95% of the other combinations. Figure 6.1 shows the best results in multiple scenarios.
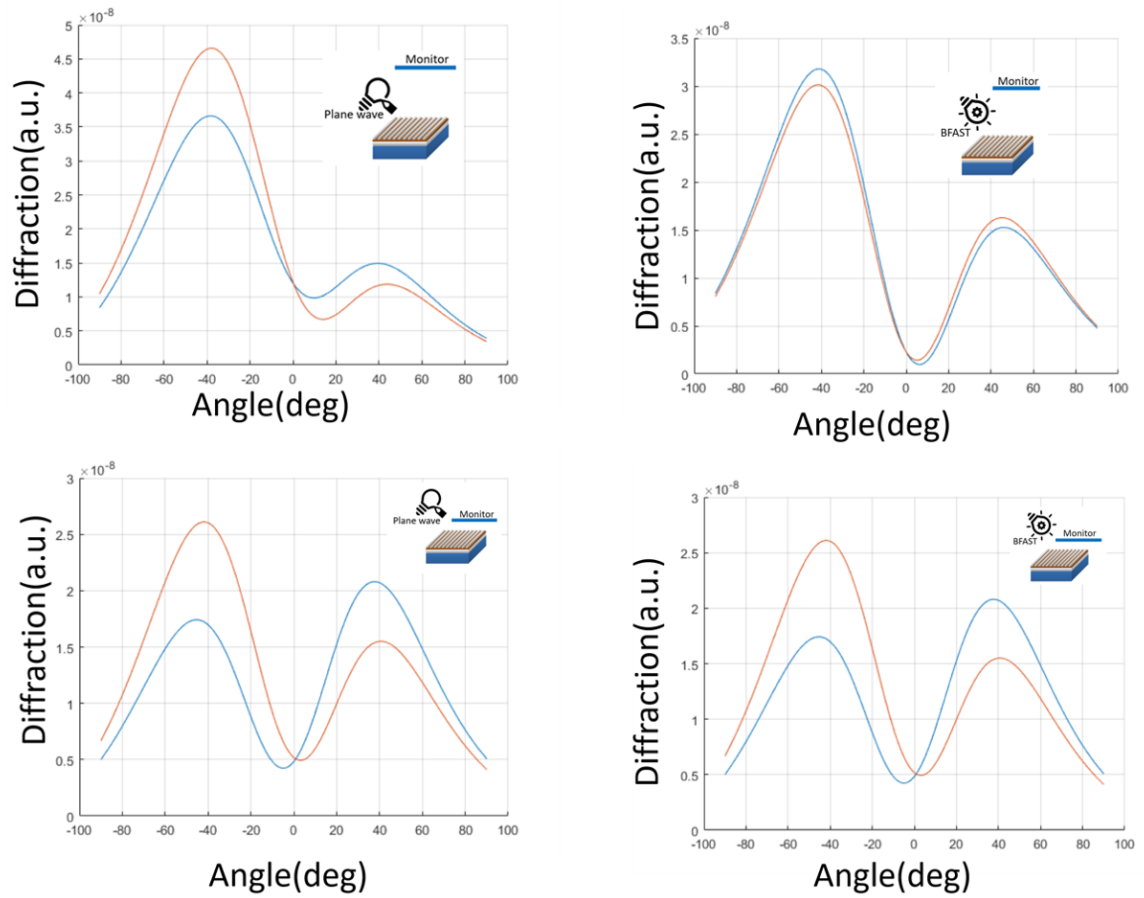
Figure 6.1 : Comparison of the FDTD results of diffractive angles of the grating structure with different simulation settings.

Bibliography

[1] B. Ouyang, G. Lan, Y. Guo, Z. Mi, and J. Song, "Phase engineering of monolayer transition-metal dichalcogenide through coupled electron doping and lattice deformation," *Applied Physics Letters*, vol. 107, no. 19, p. 191903, 2015.

[2] M. Yoshida, R. Suzuki, Y. Zhang, M. Nakano, and Y. Iwasa, "Memristive phase switching in two-dimensional 1t-tas2 crystals," *Science advances*, vol. 1, no. 9, p. e1500606, 2015.

[3] M. A. Kats, D. Sharma, J. Lin, P. Genevet, R. Blanchard, Z. Yang, M. M. Qazilbash, D. Basov, S. Ramanathan, and F. Capasso, "Ultra-thin perfect absorber employing a tunable phase change material," *Applied Physics Letters*, vol. 101, no. 22, p. 221101, 2012.

[4] D. W. Pohl, W. Denk, and M. Lanz, "Optical stethoscopy: Image recording with resolution $\lambda/20$," *Applied physics letters*, vol. 44, no. 7, pp. 651–653, 1984.

[5] S. A. Maier, *Plasmonics: fundamentals and applications.* Springer Science & Business Media, 2007.

[6] S. Lal, S. Link, and N. J. Halas, "Nano-optics from sensing to waveguiding," *Nature photonics*, vol. 1, no. 11, p. 641, 2007.

[7] A. I. Kuznetsov, A. E. Miroshnichenko, M. L. Brongersma, Y. S. Kivshar, and B. Luk'yanchuk, "Optically resonant dielectric nanostructures," *Science*,

vol. 354, no. 6314, p. aag2472, 2016.

[8] S. Makarov, A. Furasova, E. Tiguntseva, A. Hemmetter, A. Berestennikov, A. Pushkarev, A. Zakhidov, and Y. Kivshar, "Halide-perovskite resonant nanophotonics," *Advanced Optical Materials*, vol. 7, no. 1, p. 1800784, 2019.

[9] G. T. Reed, G. Mashanovich, F. Y. Gardes, and D. Thomson, "Silicon optical modulators," *Nature photonics*, vol. 4, no. 8, p. 518, 2010.

[10] M. Ferrera, N. Kinsey, A. Shaltout, C. DeVault, V. Shalaev, and A. Boltasseva, "Dynamic nanophotonics," *JOSA B*, vol. 34, no. 1, pp. 95–103, 2017.

[11] M. F. Ferreira, E. Castro-Camus, D. J. Ottaway, J. M. López-Higuera, X. Feng, W. Jin, Y. Jeong, N. Picqué, L. Tong, B. M. Reinhard, *et al.*, "Roadmap on optical sensors," *Journal of Optics*, vol. 19, no. 8, p. 083001, 2017.

[12] K. F. MacDonald, Z. L. Sámson, M. I. Stockman, and N. I. Zheludev, "Ultrafast active plasmonics," *Nature Photonics*, vol. 3, no. 1, p. 55, 2009.

[13] G. Li, S. Chen, W. Wong, E. Pun, and K. Cheah, "Highly flexible near-infrared metamaterials," *Optics express*, vol. 20, no. 1, pp. 397–402, 2012.

[14] A. Di Falco, M. Ploschner, and T. F. Krauss, "Flexible metamaterials at visible wavelengths," *New Journal of Physics*, vol. 12, no. 11, p. 113006, 2010.

[15] N. Yu, P. Genevet, M. A. Kats, F. Aieta, J.-P. Tetienne, F. Capasso, and Z. Gaburro, "Light propagation with phase discontinuities: generalized laws of reflection and refraction," *science*, vol. 334, no. 6054, pp. 333–337, 2011.

[16] N. Strohfeldt, A. Tittl, M. Schaferling, F. Neubrech, U. Kreibig, R. Griessen, and H. Giessen, "Yttrium hydride nanoantennas for active plasmonics," *Nano*

letters, vol. 14, no. 3, pp. 1140–1147, 2014.

[17] A. N. Tait, M. A. Nahmias, Y. Tian, B. J. Shastri, and P. R. Prucnal, "Photonic neuromorphic signal processing and computing," in *Nanophotonic Information Physics*, pp. 183–222, Springer, 2014.

[18] J. Hasler and H. B. Marr, "Finding a roadmap to achieve large neuromorphic hardware systems," *Frontiers in neuroscience*, vol. 7, p. 118, 2013.

[19] M. Miscuglio, A. Mehrabian, Z. Hu, S. I. Azzam, J. George, A. V. Kildishev, M. Pelton, and V. J. Sorger, "All-optical nonlinear activation function for photonic neural networks," *Optical Materials Express*, vol. 8, no. 12, pp. 3851–3863, 2018.

[20] J. M. Zurada, *Introduction to artificial neural systems*, vol. 8. West publishing company St. Paul, 1992.

[21] Y. LeCun, Y. Bengio, and G. Hinton, "Deep learning," *nature*, vol. 521, no. 7553, p. 436, 2015.

[22] M. H. Tahersima, K. Kojima, T. Koike-Akino, D. Jha, B. Wang, C. Lin, and K. Parsons, "Deep neural network inverse design of integrated nanophotonic devices," *arXiv preprint arXiv:1809.03555*, 2018.

[23] V. Sharma, S. Rai, and A. Dev, "A comprehensive study of artificial neural networks," *International Journal of Advanced research in computer science and software engineering*, vol. 2, no. 10, 2012.

[24] D. Woods and T. J. Naughton, "Optical computing: Photonic neural networks," *Nature Physics*, vol. 8, no. 4, p. 257, 2012.

[25] J. K. George, A. Mehrabian, R. Amin, J. Meng, T. F. De Lima, A. N. Tait, B. J. Shastri, T. El-Ghazawi, P. R. Prucnal, and V. J. Sorger, "Neuromorphic photonics with electro-absorption modulators," *Optics express*, vol. 27, no. 4, pp. 5181–5191, 2019.

[26] X. Lin, Y. Rivenson, N. T. Yardimci, M. Veli, Y. Luo, M. Jarrahi, and A. Ozcan, "All-optical machine learning using diffractive deep neural networks," *Science*, vol. 361, no. 6406, pp. 1004–1008, 2018.

[27] L. Novotny and B. Hecht, *Principles of nano-optics*. Cambridge university press, 2012.

[28] A. I. Kuznetsov, A. E. Miroshnichenko, Y. H. Fu, J. Zhang, and B. Luk'Yanchuk, "Magnetic light," *Scientific reports*, vol. 2, p. 492, 2012.

[29] C. Argyropoulos, N. M. Estakhri, F. Monticone, and A. Alù, "Negative refraction, gain and nonlinear effects in hyperbolic metamaterials," *Optics express*, vol. 21, no. 12, pp. 15037–15047, 2013.

[30] D. R. Abujetas, R. Paniagua-Domínguez, and J. A. Sánchez-Gil, "Unraveling the janus role of mie resonances and leaky/guided modes in semiconductor nanowire absorption for enhanced light harvesting," *ACS Photonics*, vol. 2, no. 7, pp. 921–929, 2015.

[31] J. D. Caldwell, I. Aharonovich, G. Cassabois, J. H. Edgar, B. Gil, and D. Basov, "Photonics with hexagonal boron nitride," *Nature*, vol. 41578, pp. 019–0124, 2019.

[32] L. Ju, B. Geng, J. Horng, C. Girit, M. Martin, Z. Hao, H. A. Bechtel, X. Liang,

A. Zettl, Y. R. Shen, *et al.*, "Graphene plasmonics for tunable terahertz meta-materials," *Nature nanotechnology*, vol. 6, no. 10, p. 630, 2011.

[33] S. Manzeli, D. Ovchinnikov, D. Pasquier, O. V. Yazyev, and A. Kis, "2d transition metal dichalcogenides," *Nature Reviews Materials*, vol. 2, no. 8, p. 17033, 2017.

[34] D. Wu, Y. Ma, Y. Niu, Q. Liu, T. Dong, S. Zhang, J. Niu, H. Zhou, J. Wei, Y. Wang, *et al.*, "Ultrabroadband photosensitivity from visible to terahertz at room temperature," *Science advances*, vol. 4, no. 8, p. eaao3057, 2018.

[35] J. Wilson, F. Di Salvo, and S. Mahajan, "Charge-density waves in metallic, layered, transition-metal dichalcogenides," *Physical review letters*, vol. 32, no. 16, p. 882, 1974.

[36] Y. Yu, F. Yang, X. F. Lu, Y. J. Yan, Y.-H. Cho, L. Ma, X. Niu, S. Kim, Y.-W. Son, D. Feng, *et al.*, "Gate-tunable phase transitions in thin flakes of 1t-tas 2," *Nature nanotechnology*, vol. 10, no. 3, p. 270, 2015.

[37] T. Ritschel, J. Trinckauf, G. Garbarino, M. Hanfland, M. v. Zimmermann, H. Berger, B. Büchner, and J. Geck, "Pressure dependence of the charge density wave in 1 t-tas 2 and its relation to superconductivity," *Physical Review B*, vol. 87, no. 12, p. 125135, 2013.

[38] R. Zhao, Y. Wang, D. Deng, X. Luo, W. J. Lu, Y.-P. Sun, Z.-K. Liu, L.-Q. Chen, and J. Robinson, "Tuning phase transitions in 1t-tas2 via the substrate," *Nano letters*, vol. 17, no. 6, pp. 3471–3477, 2017.

[39] C. Zhu, Y. Chen, F. Liu, S. Zheng, X. Li, A. Chaturvedi, J. Zhou, Q. Fu, Y. He,

Q. Zeng, *et al.*, "Light-tunable 1t-tas2 charge-density-wave oscillators," *ACS nano*, vol. 12, no. 11, pp. 11203–11210, 2018.

[40] K. S. Novoselov, A. K. Geim, S. V. Morozov, D. Jiang, Y. Zhang, S. V. Dubonos, I. V. Grigorieva, and A. A. Firsov, "Electric field effect in atomically thin carbon films," *science*, vol. 306, no. 5696, pp. 666–669, 2004.

[41] K. S. Novoselov, D. Jiang, F. Schedin, T. Booth, V. Khotkevich, S. Morozov, and A. K. Geim, "Two-dimensional atomic crystals," *Proceedings of the National Academy of Sciences*, vol. 102, no. 30, pp. 10451–10453, 2005.

[42] J. Qiao, X. Kong, Z.-X. Hu, F. Yang, and W. Ji, "High-mobility transport anisotropy and linear dichroism in few-layer black phosphorus," *Nature communications*, vol. 5, p. 4475, 2014.

[43] C. Slough, W. McNairy, R. Coleman, J. Garnaes, C. Prater, and P. Hansma, "Atomic force microscopy and scanning tunneling microscopy of charge-density waves in 1t-tase 2 and 1t-tas 2," *Physical Review B*, vol. 42, no. 14, p. 9255, 1990.

[44] W. Li and G. V. Naik, "In-plane electrical bias tunable optical properties of 1t-tas 2," *Optical Materials Express*, vol. 9, no. 2, pp. 497–503, 2019.

[45] R. C. Hollins, "Materials for optical limiters," *Current opinion in solid state and materials science*, vol. 4, no. 2, pp. 189–196, 1999.

[46] R. Hollins, "Overview of nonlinear optical materials research at dera," *Proc. Soc. Photo-Instrumentation Engineers*, vol. 3282, pp. 1–12, 1998.

[47] Q. Li, C. Liu, Z. Liu, and Q. Gong, "Broadband optical limiting and two-photon absorption properties of colloidal gaas nanocrystals," *Optics express*, vol. 13, no. 6, pp. 1833–1838, 2005.